Biotechnology Advances 30 (2012) 1551–1561

Contents lists available at SciVerse ScienceDirect

Biotechnology Advances

journal homepage: www.elsevier.com/locate/biotechadv

Research review paper

# Recent advances in synthesis and surface modification of lanthanide-doped upconversion nanoparticles for biomedical applications

Min Lin [a,b], Ying Zhao [b], ShuQi Wang [c], Ming Liu [d], ZhenFeng Duan [e], YongMei Chen [b,f], Fei Li [b,f], Feng Xu [a,b,*], TianJian Lu [b,**]

[a] The Key Laboratory of Biomedical Information Engineering of Ministry of Education, School of Life Science and Technology, Xi'an Jiaotong University, Xi'an, PR China
[b] Biomedical Engineering and Biomechanics Center, Xi'an Jiaotong University, Xi'an, PR China
[c] Brigham and Women's Hospital, Harvard Medical School, Boston, MA, USA
[d] Electrical and Computer Engineering Department, Northeastern University, Boston, MA, USA
[e] Center for Sarcoma and Connective Tissue Oncology, Massachusetts General Hospital, Harvard Medical School, MA, USA
[f] Department of Chemistry, School of Science, Xi'an Jiaotong University, Xi'an, PR China

ARTICLE INFO

Available online 27 April 2012

*Keywords:*
Lanthanide-doped upconversion nanoparticles
Synthesis
Surface modification
Biomedical applications

ABSTRACT

Lanthanide (Ln)-doped upconversion nanoparticles (UCNPs) with appropriate surface modification can be used for a wide range of biomedical applications such as bio-detection, cancer therapy, bio-labeling, fluorescence imaging, magnetic resonance imaging and drug delivery. The upconversion phenomenon exhibited by Ln-doped UCNPs renders them tremendous advantages in biological applications over other types of fluorescent materials (*e.g.*, organic dyes, fluorescent proteins, gold nanoparticles, quantum dots, and luminescent transition metal complexes) for: (i) enhanced tissue penetration depths achieved by near-infrared (NIR) excitation; (ii) improved stability against photobleaching, photoblinking and photochemical degradation; (iii) non-photodamaging to DNA/RNA due to lower excitation light energy; (iv) lower cytotoxicity; and (v) higher detection sensitivity. Ln-doped UCNPs are therefore attracting increasing attentions in recent years. In this review, we present recent advances in the synthesis of Ln-doped UCNPs and their surface modification, as well as their emerging applications in biomedicine. The future prospects of Ln-doped UCNPs for biomedical applications are also discussed.



**Contents**



* Corresponding author at: The Key Laboratory of Biomedical Information Engineering of Ministry of Education, School of Life Science and Technology, Xi'an Jiaotong University, Xi'an, PR China.
** Corresponding author.
*E-mail addresses:* fengxu@mail.xjtu.edu.cn (F. Xu), tjlu@xjtu.edu.cn (T. Lu).

0734-9750/$ – see front matter © 2012 Elsevier Inc. All rights reserved.
doi:10.1016/j.biotechadv.2012.04.009

## 1. Introduction

Due to high temporal and spatial resolutions, fluorescence imaging is an important and challenging technique for *in vitro* and *in vivo* biological studies and clinical applications (Berezin and Achilefu, 2010; Kobayashi et al., 2010; Louie, 2010). Conventional fluorophores (*e.g.*, organic fluorophores, quantum dots, fluorescent proteins and luminescent transition metal complexes) have been widely used as luminescent reporters for biological applications (Lau et al., 2009; Malkani and Schmid, 2011; Medintz et al., 2005; Wang et al., 2009a; Yu et al., 2008; Zhao et al., 2010). Nevertheless, conventional fluorophores are associated with several limitations, such as low photostability, auto-fluorescence, cytotoxicity and limited detection sensitivity (Hilderbrand et al., 2009; Larson et al., 2003; van de Rijke et al., 2001; Wang and Liu, 2008). Lanthanide (Ln)-doped upconversion nanoparticles (UCNPs) exhibit unique fluorescent property known as photon upconversion, providing tremendous advantages over conventional fluorophores for biomedical applications. These advantages include (i) enhanced penetration depth into tissues upon NIR excitation (Chatterjee et al., 2008); (ii) significantly decreased auto-fluorescence from surrounding tissues (Idris et al., 2009; Johnson et al., 2010; Wu et al., 2011); (iii) non-photobleaching, non-photoblinking and high spatial resolution during bioimaging (Idris et al., 2009; Park et al., 2009; Sudhagar et al., 2011); (iv) decreased photo-damage to biological specimens (*e.g.*, RNA, DNA) due to lower energy NIR excitation (Jiang and Zhang, 2010); (v) low-cytotoxic to a broad range of cell lines (Chatterjee et al., 2008; Jalil and Zhang, 2008; Park et al., 2009; Tsien, 1998; Wang et al., 2006; Xiong et al., 2009, 2010). Hence, Ln-doped UCNPs hold great potential as novel fluorophores for biological applications.

This review aims to present the state-of-the-art in the synthesis and surface modification of Ln-doped UCNPs and their emerging biological applications. In Section 2, we describe basic principle underlying the phenomenon of upconversion and the corresponding crystalline structure of Ln-doped UCNPs. Section 3 presents popular chemical approaches for the synthesis of Ln-doped UCNPs with well controlled size distribution, morphologies, and luminescent properties. Advantages and disadvantages associated with each synthetic method are discussed. Section 4 focuses on the general surface modification strategies of Ln-doped UCNPs for enhanced luminescence and improved solubility in solvent facilitating further biological applications. The applications of Ln-doped UCNPs for *in vitro* and *in vivo* imaging, biological sensing, detection, development of point-of-care devices and drug delivery are discussed in Section 5. Section 6 highlights future research topics associated with Ln-doped UCNPs.

## 2. Upconversion mechanism and construction of UCNPs

### 2.1. Mechanism of upconversion

Conventional fluorophores exhibit the phenomenon of downconversion, *i.e.*, higher energy photons are absorbed while lower energy ones are emitted due to internal energy loss (IEL) (Lakowicz, 2006) (Fig. 1a). Compared with downconversion, upconversion is a process that causes the emission of higher energy photons through sequential absorption of lower energy photons (Auzel, 2004). The mechanism underlying upconversion process has been extensively explored and is generally divided into three classes (Wang and Liu, 2009; Wang et al., 2011b), *i.e.*, excited state absorption (ESA), energy transfer upconversion (ETU), and photon avalanche (PA). In comparison with the other two processes, ETU has been widely employed to obtain high upconversion efficiency (emission density versus NIR excitation power), involving the absorption of a pump phonon of the same energy by each of the two neighboring ions (Fig. 1b). A subsequent non-radiative energy transfer promotes one of the ions to an upper energy level (EL2) while the other ion relaxes back to the ground state (GS). The relaxation from EL2 results in the emission of higher energy photons.

### 2.2. Ln-doped UCNPs

Ln-doped UCNPs are typically composed of an inorganic host lattice and trivalent lanthanide dopant ions embedded in the host lattice. Host lattice is a transparent crystalline that accommodates the dopants. Several criteria need to be fulfilled for choosing the host lattice as reviewed by Wang and Liu (2009) and by Ong et al. (2010): (i) close lattice matches to dopant ions; (ii) low phonon vibration energies; (iii) good chemical stability. Based on these criteria, the most commonly used host lattice for the synthesis of Ln-doped UCNPs are fluorides (Liang et al., 2011; Sudheendra et al., 2011; Yu et al., 2010) and oxides (Kamimura et al., 2008; Singh et al., 2010; Yang et al., 2009). So far, fluoride-based (*i.e.*, $NaYF_4$) UCNPs have been identified as one of the most efficient upconversion fluorescent nanoparticles due to their low phonon vibration energy (Boyer et al., 2007; Heer et al., 2004; Yi and Chow, 2007).

To enhance the luminescence efficiency of Ln-doped UCNPs, two types of dopant ions are needed. One that emits visible light is called an activator, while the other acting as the donator of energy is the sensitizer. To minimize cross-relaxation energy loss, the concentration of the sensitizer is relatively high (~20 mol%), while for the activator, the concentration is below 2 mol% (Wang and Liu, 2009). The dopant selection criterion is based on characteristic spaced energy levels that render photon absorption by sensitizer and subsequent energy transfer between the sensitizer and activator in the upconversion process. With high absorption coefficient and upconversion efficiency, $Yb^{3+}$ is usually selected as the sensitizer (Soukka et al., 2008). $Er^{3+}$, $Tm^{3+}$, and $Ho^{3+}$ are good candidates as activators, which possess ladder-like energy levels and are well resonant with non-

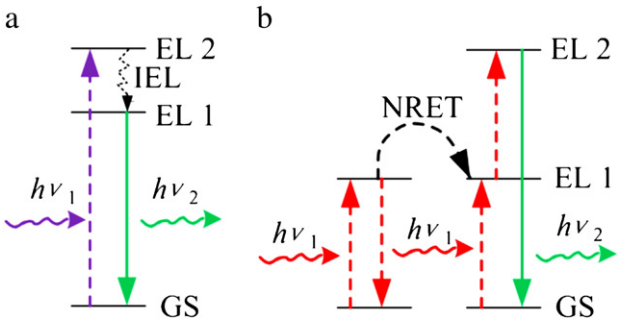


**Fig. 1.** Illustration of (a) downconversion and (b) energy transfer upconversion mechanism. IEL: internal energy loss; GS: ground state; EL: energy level; NRET: non-radiative energy transfer; $h\nu_1$: incident light; $h\nu_2$: emission light.

radiative multiphonon relaxation from $Yb^{3+}$, enabling efficient energy transfer from $Yb^{3+}$ to these ions (Wang and Liu, 2009). Other lanthanide ions, such as Tb3+ (Liang et al., 2009), Pr3+ and $Dy^{3+}$ (Lakshminarayana et al., 2008) have also been used as activators. Typical lanthanide host-dopant systems and major emissions are listed in Table 1.

## 3. Synthesis of Ln-doped UCNPs

Ln-doped UCNPs size, crystalline phase purity, morphology and monodispersity are critical parameters that directly influence the upconversion fluorescent properties (*e.g.*, upconversion efficiency, emitting light wavelength) (Shan and Ju, 2009; Wang et al., 2010b; Zhang et al., 2009a). Great efforts have been dedicated to developing a variety of chemical approaches for synthesis of Ln-doped UCNPs (Wang and Liu, 2009; Wang et al., 2011b; Zhang et al., 2010a). Representative Ln-doped UCNPs synthetic methods such as co-precipitation, thermal decomposition, sol–gel processing and hydro(solvo)thermal method are discussed below.

### 3.1. Co-precipitation method

The co-precipitation synthetic method is simple in the sense that it is not time consuming and does not require costly setup, complex procedures, or severe reaction conditions (Du et al., 2011). Nanoparticle growth can be controlled and stabilized by adding capping ligands such as polyvinylpyrrolidone (PVP), polyethylenimine (PEI) (Wang et al., 2006; Wu et al., 2002) and ethylenediaminetetraacetic acid (EDTA) (Yi et al., 2004) into the solvent. However, in rare cases, crystalline nanoparticles formed directly from co-precipitation (Du et al., 2011), requiring post heat treatment (Su et al., 2009; Xu et al., 2010). It has been reported that hexagonal-phase $NaYF_4$:Yb,Er nanocrystals exhibit an upconversion efficiency higher than cubic-phase $NaYF_4$:Yb,Er (Wang et al., 2010b). Co-precipitation generally yields cubic-phase $NaYF_4$:Yb,Er which is not an efficient upconverter. Subsequent calcination at high temperatures results in sharpened crystal structure or partial phase transfer to hexagonal-phase $NaYF_4$:Yb,Er that has a higher upconversion efficiency (Yi et al., 2004). In addition to $NaYF_4$:Yb,Er nanocrystals, $LuPO_4$:Yb,Tm and $YbPO_4$:Er,Tm nanocrystals have also been synthesized *via* co-precipitation and subsequently heat treatment for improved upconversion emission (Xu et al., 2009).

### 3.2. Thermal decomposition

Thermal decomposition is another widely used technique, which involves dissolving organic precursors in high-boiling-point solvents (*e.g.*, oleic acid (OA), oleylamine (OM), octadecene (ODE)) for the synthesis of highly monodispersed UCNPs (Boyer et al., 2006, 2007; Liu et al., 2009b; Mahalingam et al., 2009). In this method, rare earth trifluoroacetates are thermolyzed in the presence of high-boiling-point solvents at a temperature usually exceeding 300 °C. Using this method, Yan's group has done a pioneer work on the synthesis of Ln-doped UCNPs (Du et al., 2009; Mai et al., 2006, 2007; Yin et al., 2010; Zhang et al., 2010a). For example, $Er^{3+}$, $Yb^{3+}$ and $Tm^{3+}$, $Yb^{3+}$ doped monodispersed cubic-phase and hexagonal-phase $NaYF_4$ nanocrystals have been synthesized by thermal decomposition of trifluoroacetate precursors in OA/OM/ODE solvents and OA/ODE solvents, respectively (Mai et al., 2006). $NaYF_4$-based UCNPs with different luminescent properties have also been obtained with similar synthetic methods (Mai et al., 2007; Yin et al., 2010). They have also extended the synthetic route for synthesis of $LiYF_4$ and $KGdF_4$ UCNPs with $Li(CF_3COO)$ and $K(CF_3COO)$ used instead as one of the precursors (Du et al., 2009). Alternatively, by decomposing the precursors of $Na(CF_3COO)$, $Y(CF_3COO)_3$, $Yb(CF_3COO)_3$, and $Er(CF_3COO)_3$/$Tm(CF_3COO)_3$ in OM solvent under 330 °C, hexagonal-phase $NaYF_4$:Yb,Er and $NaYF_4$:Yb,Tm nanoparticles with an average particle size of 10.5 nm and much higher upconversion fluorescence intensity than that of cubic-phase $NaYF_4$:Yb,Er nanocrystals were obtained (Yi and Chow, 2006). However, the disadvantages associated with this method are the use of expensive and air-sensitive metal precursors (Mader et al., 2010; Wang et al., 2010b, 2011d), and the generation of toxic by-products (Mahalingam et al., 2009; Yi and Chow, 2006).

### 3.3. Sol–gel process

The sol–gel process features the hydrolysis and polycondensation of metal acetate or metal alkoxide based precursors (Liu et al., 2009b; Patra et al., 2002). Various metal oxide based Ln-doped UCNPs such as $YVO_4$:Yb,Er, $Lu_3Ga_5O_{12}$:Er, $BaTiO_3$:Er, $TiO_2$:Er and $ZrO_2$:Er, have been prepared using the sol–gel method (Li et al., 2008a; Liu et al., 2009b; Patra et al., 2002, 2003; Quan et al., 2009). Despite its success in the synthesis of various Ln-doped UCNPs, the sol–gel method has limited control over synthesized particle size, and particle aggregation may occur when dispersed in aqueous solutions during biological

**Table 1**
Representative UCNPs with different host-dopant systems, excitation wavelengths and emission peaks.

| Dopant ions | | | Major emissions (nm) | | | |
|---|---|---|---|---|---|---|
| Host lattice | Sensitizer | Activator | Blue | Green | Red | Ref. |
| $NaYF_4$ | Yb | Er | | 518, 537 | 652 | Wang et al. (2005) and Yi et al. (2004) |
| | Yb | Er | | 540 | 660 | Heer et al. (2004) |
| | Yb | Er | | 510–530 | 635–675 | Liu et al. (2009a) |
| | Yb | Er | | 521,539 | 651 | Li and Zhang (2008) |
| | Yb | Tm | 450, 475 | | 647 | Heer et al. (2004) |
| | Yb | Er, Tm | 499, 474 | 525 | 644, 693 | Wang and Liu (2008) |
| | Yb | Ho | | 540 | | Ehlert et al. (2008) |
| | Yb | Ho | | 542 | 645, 658 | Shan et al. (2007) |
| $LaF_3$ | Yb | Tm | 475 | | | Liu and Chen (2007) |
| | Yb | Er | | 520, 545 | 659 | Liu and Chen (2007) |
| | Yb | Ho | | 542 | 645, 658 | Liu and Chen (2007) |
| $CaF_2$ | Yb | Er | | 524 | 654 | Wang et al. (2009b) |
| $Y_2O_3$ | Yb | Er | | 550 | 660 | Kamimura et al. (2008) |
| | Yb | Ho | | 543 | 665 | Qin et al. (2007) |
| $Lu_2O_3$ | Yb | Er, Tm | 490 | 540 | 662 | Yang et al. (2009) |
| $LuPO_4$ | Yb | Tm | 475 | | 649 | Heer et al. (2003) |

All are under NIR (980 nm) excitation.

applications. Furthermore, post heat treatment is often needed to improve crystalline phase purity for enhanced luminescence efficiency. However, the extra heat treatment may induce unwanted particle aggregation.

### 3.4. Hydro(solvo)thermal method

The solubility of solids is greatly improved under hydro(solvo) thermal conditions (*e.g.*, reaction temperature rises above a critical point, pressurized solvent), which accelerates reactions between solids (Chuai et al., 2011; Du et al., 2011; Feng and Xu, 2001; Huang et al., 2010). This approach allows for the synthesis of highly crystalline nanocrystals with tunable size, morphology, optical and magnetic properties *via* controlled reaction temperature/time, concentration, pH value, precursors etc. (Guo et al., 2010; Niu et al., 2011; Yan and Yan, 2008; Zhang et al., 2009a). In addition to convenient size and morphology control, the superiority of this method over other synthetic methods lies in the "one-pot process": with heat-resistant polymer (*e.g.*, PEI, PVP) added into the solvent (Liu et al., 2009b; Wang et al., 2006), uniform-sized nanoparticles with appropriate surface modification could be obtained through a single reaction process (Wang et al., 2010c). Nevertheless, the main challenge of the hydro (solo)thermal method is the impossibility of observing the nanocrystals growth processes.

In addition to the methods described above, other procedures such as microwave-assisted synthesis (Patra et al., 2005; Vadivel Murugan et al., 2006), combustion synthesis (Gallini et al., 2005; Shan and Ju, 2009; Vu et al., 2007) and hydrothermal *in situ* conversion route (Heer et al., 2003; Yi and Chow, 2005) have also been employed for fabricating Ln-doped UCNPs. The advantages and disadvantages of various synthetic routes are summarized in Table 2. Among them, the hydro(solvo)thermal reaction method is the most widely used due to easy and precise control of the shape and size of Ln-doped UCNPs (Yan and Yan, 2008). The reaction conditions, such as reaction time, concentration, temperature, pH value, and surfactant involved in hydro(solvo)thermal procedures can be fine-tuned to tailor the optical and magnetic properties for specific biological applications.

## 4. Surface modification of Ln-doped UCNPs

For many biomaterials, surface fictionalization is critical for fulfilling their biological functions (Williams, 2011). Surface modification of Ln-doped UCNPs is required in biosciences, such as immunoassay (Niedbala et al., 2001), targeted imaging (Hu et al., 2009; Xiong et al., 2009), nucleic acid encoding (Zhang et al., 2011), cancer therapy (Wang et al., 2011a) and bio-detection (van de Rijke et al., 2001). The understanding of surface modification of Ln-doped UCNPs is vital for improving the upconversion efficiency and aqueous solubility as well as providing potential capabilities for different biomedical applications (Ghosh et al., 2009; Yi and Chow, 2007).

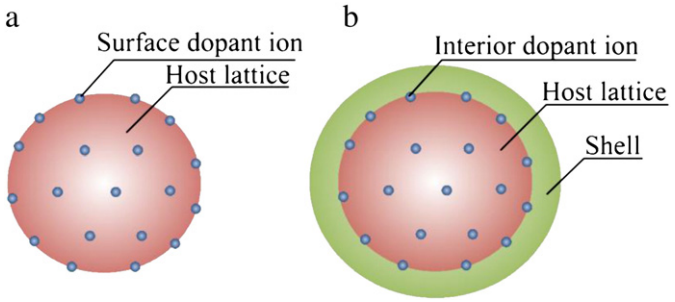


**Fig. 2.** (a) Illustration of lanthanide-doped UCNPs with large proportion of surface dopant ions; (b) dopant ions confined in the interior of a core/shell structure by surface coating of Ln-doped UCNPs.

### 4.1. Surface coating for enhanced upconversion efficiency

A large proportion of surface dopant ions exists in nano-sized Ln-doped UCNPs (Fig. 2a). Non-radiative energy loss occurs due to lack of protection by the host lattice, resulting in low efficiency of upconversion luminescence as compared with bulk materials (Yi et al., 2004). Such limitation could be avoided through coating an inert crystalline shell onto the surface of doped nanocrystals. In such core/shell structures, the dopant ions are confined in the interior core of the nanocrystals (Fig. 2b). The shell could effectively suppress energy loss on the crystal surface, leading to enhanced luminescence efficiency. For instance, significant upconversion luminescence enhancements of ~7 times for $NaYF_4$:Yb,Er and ~29 times for $NaYF_4$:Yb,Tm have been achieved by decorating with ~2 nm thick undoped $NaYF_4$ shell (Yi and Chow, 2007). Whereas, Mai et al. (2007) found only 1/2–1 folds luminescent increase for $NaYF_4$ coated $NaYF_4$:Yb,Er UCNPs. Increases of over 20 folds in upconversion efficiency have been observed by coating undoped $KYF_4$ on the surface of $KYF_4$:Yb,Er nanocrystals (Schäfer et al., 2008). $NaGdF_4$:Er,Yb nanoparticles coated with a shell of $NaGdF_4$ have also been found to exhibit greatly improved luminescent intensity as compared with uncoated ones (Vetrone et al., 2009). In addition to coating with materials that have the same composition with the host lattice, amorphous shells or carbonized glucose shells have been found to be useful for improving the luminescence efficiency of Ln-doped UCNPs (Li and Zhang, 2006; Li et al., 2010).

**Table 2**
Advantages and disadvantages of typical synthetic routes for UCNPs.

| Method | Examples (hosts) | Advantages | Disadvantages | Ref. |
|---|---|---|---|---|
| Co-precipitation | $Y_3Al_5O_{12}$, $BaYF_5$, $NaYF_4$, LuPO4, $YbPO_4$ | Fast synthesis, low cost and simple procedures | Lack of particle size control, considerable aggregation, high temperature calcination typically needed | Du et al. (2011), Su et al. (2009) and Xu et al. (2009) |
| Thermal decomposition | $LiYF_4$, $NaYF_4$ | High quality, monodispersed nanocrystals | Expensive, air-sensitive metal precursors, toxic by-products | Lim (2009), Mahalingam et al. (2009), Wang et al. (2006) and Yi and Chow (2006) |
| Sol–gel processing | $YVO_4$, $Lu_3Ga_5O_{12}$, $BaTiO_3$, $TiO_2$ $ZrO_2$ | Cheap precursors | High temperature calcination needed, considerable particle aggregation | Li et al. (2008a), Liu et al. (2009b), Patra et al. (2002, 2003) and Quan et al. (2009) |
| Combustion synthesis | $Y_2O_3$, $LaPO_4$, $La_2O_2S$ | Fast synthesis, energy saving | Considerable aggregation, lack of particle size control, low purity | Gallini et al. (2005), Shan and Ju (2009) and Vu et al. (2007) |
| Flame synthesis | $Y_2O_3$, $La_2O_3$, $Gd_2O_3$ | Fast synthesis, large scale | Considerable aggregation, lack of particle size control, low purity | Hilderbrand et al. (2009) and Wang and Liu (2008) |
| Hydro(solvo) thermal synthesis | $LuF_3$, $NaYF_4$, $Ba_2YF_7$, $ZnGa_2O_4$, $YVO_4$ | High quality crystals with controllable particle size, shape and dopant ion concentrations | Impossibility of observing the nanocrystal growth processes | Chuai et al. (2011), Huang et al. (2010), J alil and Zhang (2008), Su Kim et al. (2007) and Venkatramu et al. (2008) |

However, while the luminescence intensities can be tuned by varying the thickness of amorphous shells, the increase in luminescence is limited due to high-energy oscillations from the amorphous shells.

### 4.2. Surface functionalization for biomedical applications

In addition to high upconversion luminescence efficiency, the preparation of water soluble Ln-doped UCNPs is crucial for biological applications. Most Ln-doped UCNPs synthesized from high-temperature approaches discussed in Section 2 have limitations on both aqueous solubility and biological functions. Surface functionalization with hydrophilic ligands is required prior to exploring various bioanalytical potentials. Five major strategies have been proposed to enable the water solubility and biofunctionality of Ln-doped UCNPs (Wang and Liu, 2009): (1) surface silanization; (2) ligand exchange; (3) ligand oxidation; (4) ligand attraction; (5) electrostatic layer by layer assembly.

Among various surface functionalization methods, surface silanization is the most commonly applied for two reasons: (i) well established chemical approaches of silica coating, and (ii) silica coating is readily applicable to both hydrophilic and hydrophobic nanoparticles (Liu and Han, 2010; Piao et al., 2008). For instances, Johnson et al. (2010) reported silica coating on PVP stabilized $NaYF_4$:Yb,Er nanocrystals in ethanol. With PVP stabilized $NaYF_4$:Yb,Er nanocrystals dispersed in ethanol, PVP on the surface of the nanocrystals facilitates both stability in ethanol and affinity with silica allowing uniform growing of silica shell with thickness of ~9 nm. Using a similar method, Li and Zhang (2006) prepared water soluble silica coated PVP stabilized $NaYF_4$:Yb,Er nanocrystals: the thickness of silica shells could be varied from 10 nm to 1 nm by adjusting the concentration of precursor for silica formation, *i.e.*, tetraethoxysilane (TEOS).

Apart from surface silanization, alternative ways for surface functionalization of Ln-doped UCNPs have been developed by surface modification with non-silane reagents. For example, Chatterjee et al. (2008) directly coated Ln-doped UCNPs with a layer of PEI *via* a modified hydrothermal synthesis. Layer-by-layer (LBL) assembly strategy has also been employed for functionalization of Ln-doped UCNPs. *Via* electrostatic attraction, Hilderbrand et al. (2009) coated the nanoparticles with a layer of polyacrylic acid (PAA): carboxyl groups of the PAA was covalently linked with amino-modified polyethylene glycol (PEG), resulting in hydrophilic and functional Ln-doped UCNPs. In addition to LBL assembly strategy, ligand-exchange method has been demonstrated as a facile approach for surface functionalization of Ln-doped UCNPs (Qiu et al., 2011; Zhou et al., 2011). For example, Yi and Chow (2006) prepared water soluble $NaYF_4$:Yb,Er nanoparticles using a ligand exchange method. In their study, Ln-doped UCNPs were firstly stabilized with oleylamine ligands; the amine ligand was subsequently replaced by bifunctional organic molecules, providing water soluble surface. To fine-tune the surface properties of Ln-doped UCNPs for a controlled cell–nanoparticle interaction, Jin et al. (2011) prepared PEI and PAA coated Ln-doped UCNPs by ligand exchange of PVP with PEI or PAA due to their higher binding affinity toward lanthanide ions than PVP.

## 5. Advantages of Ln-doped UCNPs in biomedical applications

With unique upconversion mechanism, Ln-doped UCNPs offer high sensitivity and high signal-to-noise ratio for bioimaging and bio-detection. Furthermore, emission in the NIR region with NIR excitation enables deep tissue reaching while avoiding photodamaging to biological specimens. Such unique properties provide Ln-doped UCNPs with great potential for a wide range of biological applications, such as biological imaging, biological sensing/detection, development of point-of-care devices and drug delivery. A brief overview of the advantages associated with Ln-doped UCNPs in biological applications is presented below.

### 5.1. Biological imaging

Gold nanorods and quantum dots have been widely used for bioimaging (Huang et al., 2009; Medintz et al., 2005; Wang et al., 2010d, 2012). However, gold nanorods are incapable of deep tissue imaging due to signal attenuation, along with low contrast and auto-fluorescence (Qian et al., 2010a). Although quantum dots exhibit negligible photobleaching, greater brightness, and narrow mission bands (Xing and Rao, 2008), there are concerns about their cytotoxicity (Chatterjee et al., 2008). Ln-doped UCNPs are photostable against photobleaching and blinking (Park et al., 2009; Yu et al., 2009). Moreover, absence of auto-fluorescence (Idris et al., 2009) and deep tissue reaching resulting from luminescence after NIR excitation (Chatterjee et al., 2008) enable them as promising probes for *in vitro* and *in vivo* imaging as have been reviewed (Chatterjee et al., 2010; Mader et al., 2010). For comparison, the advantages and disadvantages of those materials and other materials used for bioimaging are listed in Table 3.

A number of studies have reported the application of Ln-doped UCNPs in *in vitro* cellular and tissue imaging. *In vitro* cellular imaging involves targeting of Ln-doped UCNPs to some subcellular components (*e.g.*, membrane proteins). *In vitro* imaging with spatial and temporal distributions of colon cancer cells (Chatterjee et al., 2008), ovarian cancer cells (Boyer et al., 2010), HeLa cells (Cheng et al., 2011; Dong et al., 2011; Jin et al., 2011; Wang et al., 2009d), myoblasts (Jalil and Zhang, 2008), glioblastoma and breast carcinoma cells (Jin et al., 2011; Xing et al., 2012; Yang et al., 2012) have been demonstrated. In a recent report by Jin et al. (2011), the brighter *in vitro* cellular imaging can be achieved by positively charged UCNPs due to their enhanced cellular uptake efficiency. Tissue imaging was firstly demonstrated by Zijlmans et al. (1999) who used $Y_2O_2S$:Yb,Tm nanoparticles to study the spatial distribution of prostate-specific antigen (PSA) in human prostate tissue. The

**Table 3**
Comparison of representative probes for bioimaging.

| Probe materials | Types | Advantages | Disadvantages | Ref. |
|---|---|---|---|---|
| Organic fluorophores | Organic dyes, fluorescent proteins | High quantum efficiency ultra-sensitive detection, high specific | Auto-fluorescence, bleaching, blinking | Jaafar et al. (2010), Weiss (1999) and Wu et al. (2002) |
| Gold | Nanorods, nanoparticle | Biocompatible | Signal attenuation in deep tissue imaging, low contrast | Huang et al. (2009) and Qian et al. (2010a) |
| Quantum dots | Colloidal II–VI semiconductor nanocrystals | High fluorescence brightness, narrow and tunable emission | Toxic, signal attenuation in deep tissue imaging | Chatterjee et al. (2008) and Jańczewski et al. (2011) |
| Luminescent transition metal complexes | Iridium(III) based metallorganic materials | Good water solubility, lack of dye–dye interactions, and large Stokes' shifts | Toxic, auto-fluorescence, signal attenuation in deep tissue imaging | Lau et al. (2009), Park et al. (2009), Yu et al. (2008) and Zhao et al. (2010) |
| Lanthanide-doped UCNPs | Lanthanide-doped fluorides and oxides | Large anti-Stokes' shifts, non-blinking, non-bleaching, non-auto-fluorescence, deep tissue reaching, good biocompatibility | Low upconversion efficiency | Chatterjee et al. (2008), Idris et al. (2009), Jalil and Zhang (2008), Park et al. (2009) and Yu et al. (2009) |

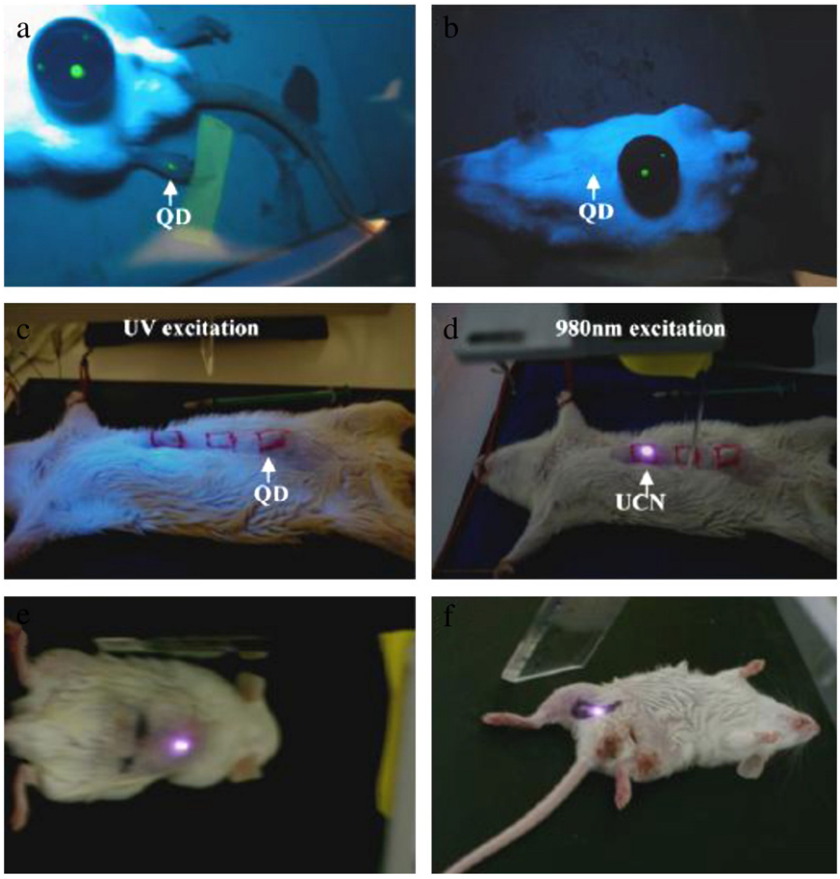


**Fig. 3.** Comparison of quantum dots with Ln-doped UCNPs in *in vivo* imaging of rat. (a–c) Quantum dots injected into foot, back and abdominal skin respectively with black disk containing quantum dots (in a, b) as control. (d–f) UCNPs injected into different regions of the rat, showing strong fluorescence intensity (Chatterjee et al., 2008).

absence of auto-fluorescence from tissue itself under NIR excitation enables high-resolution imaging.

More importantly, *in vivo* organism and animal imaging has been achieved with Ln-doped UCNPs. Lim et al. (2006) carried out pioneering work on live organism imaging by inoculating $Y_2O_3$:Yb,Er nanoparticles into live nematode *Caenorhabditis elegans* worms. The digestive system of the worm was subsequently imaged under NIR excitation, showing clearly distribution of nanoparticles in intestines. Besides organism imaging, *in vivo* animal imaging has also been demonstrated (Chatterjee et al., 2008), where $NaYF_4$:Yb,Er nanoparticles were injected underneath abdominal and back skin of anesthetized rats. Upon NIR excitation, the luminescence from Ln-doped UCNPs can be clearly observed even when the nanoparticles are located ~10 mm beneath the skin, which is far deeper than that by quantum dots as imaging probes (Fig. 3).

### 5.2. Biological sensing/detection

The capabilities of Ln-doped UCNPs in various biological sensing/detection are realized based mainly on two mechanisms: fluorescence resonance energy transfer (FRET) and non-FRET (Soukka et al., 2008; Zhang et al., 2011). The FRET process is realized when energy is transferred between the donor and the acceptor through Coulombic interactions. FRET-based detection is only possible when the distance between the donor and the acceptor is typically small (<10 nm). Based on such phenomenon, several research groups reported the applications of lanthanide-doped UCNPs in FRET-based highly sensitive detection (Rantanen et al., 2008; Wang et al., 2009c; Zhang et al., 2006, 2011).

Based on the FRET process between rabbit anti-goat immunoglobulin G (IgG) functionalized NaYF4:Yb,Er nanoparticles and human IgG functionalized gold nanoparticles, Wang et al. (2009c) demonstrated the detection of goat anti-human IgG with a limit of 0.88 μg/ml. In their study, rabbit anti-goat IgG functionalized UCNPs suspension was added into different amounts of goat anti-human IgG solutions. After incubating for 30 min, human IgG functionalized gold suspension was added subsequently into the solution mixtures. As goat anti-human IgG is able to act like a bridge to couple the two particles close enough to generate FRET under excitation (Fig. 4a). The FRET between the two particles quenches the upconversion luminescence of $NaYF_4$:Yb,Er nanoparticles. The quenching efficiency was found to be linearly correlated with the concentration of the goat anti-human IgG. Using human biotin functionalized $NaYF_4$:Yb/Er nanoparticles and gold nanoparticles to form the donor–acceptor system, Wang et al. (2005) reported the detection of avidin with a limit of 0.5 nM. Also with functionalized $NaYF_4$:Yb,Er nanoparticles and gold nanoparticles, Zhang et al. (2009b) found another application as a reversible luminescence switch to solutions having different pH values.

For non-FRET-based bio-detection, Ln-doped UCNPs were used as a luminescent reporter and the luminescence from Ln-doped UCNPs was observed directly. The non-auto-fluorescence feature of Ln-doped UCNPs offers improved detection limits as compared with conventional reporters. For example, Hampl et al. (2001) demonstrated the application of $Y_2O_2S$:Yb,Er nanoparticles in the detection of 10 pg human chorionic gonadotropin from a 100 ml sample. A comparison with conventional labels such as colloidal gold or colored latex beads showed a 10-fold improvement in sensitivity when using $Y_2O_2S$:Yb,Er nanoparticles. van de Rijke et al. (2001) also explored the usage of $Y_2O_2S$:Yb,Er nanoparticles in the detection of oligonucleotides, achieving a detection limit of 1 ng/μl which is four-fold increase in sensitivity relative to that achieved with cyanine 5 labels (Fig. 4b).

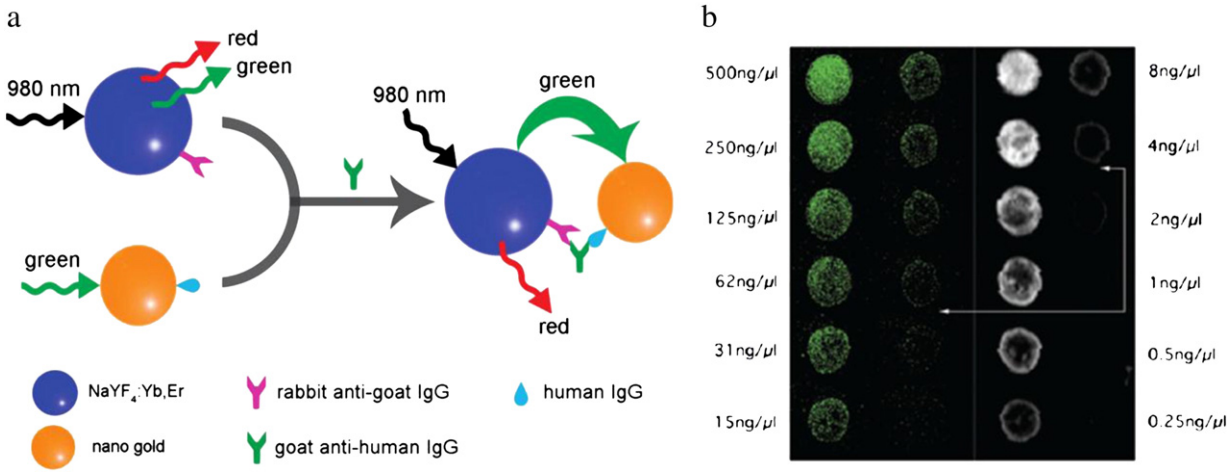


**Fig. 4.** Illustration of lanthanide-doped UCNPs in highly sensitive bio-detection. (a) Fluorescence resonance energy (FRET) based detection of goat anti-human IG using Ln-doped UCNPs as energy donor and gold nanoparticles as acceptor (Wang et al., 2009c). (b) Model low-complexity microarray hybridization with biotin HEF-DNA detected with avidin-Cy5 and laser scanning (right panel) and with functionalized UCNPs (left panel). Concentrations of HEF probe DNA solutions are shown next to the spots (500–0.25 ng/μl). The spots in the first and third columns correspond to concentrations along the left side, while that in the second and fourth columns correspond to concentrations along the right side. Detection sensitivity is indicated by the arrows (van de Rijke et al., 2001).

### 5.3. Development of point-of-care devices

Point-of-care devices have been developed to achieve rapid detection of infectious agents, cancer biomarkers and chemical analytes (Gurkan et al., 2011; Wang et al., 2010e, 2011e). These devices are cost-effective and user-friendly, which eliminates the need for bulky instruments and skilled operators (Wang et al., 2011c). Lateral flow (LF) strip is one of the most commonly used point-of-care devices relying on the use of gold nanoparticles or latex beads. Although the results can be detected with naked eyes, LF strips have limited use due to the lack of sensitivity, especially at the early stage of infectious diseases where the analyte concentration is relatively low. Thus, further improvement needs to be made in LF assays to increase the sensitivity for early detection of biological biomarkers.

With fast testing speed (<10 min) (Niedbala et al., 2001) and extraordinarily high sensitivity (Wang and Li, 2006; Zuiderwijk et al., 2003), Ln-doped UCNPs are attractive for the development of point-of-care devices. A typical example was shown by Niedbala et al. (2001) who designed LF assay strips for drug abuse testing (Fig. 5). In this assay, functionalized Ln-doped UCNPs were used to replace colloidal gold or latex particles. Because of the capacity to emit multiple colors, Ln-doped UCNPs were used for simultaneous detection of amphetamine, phencyclidine and methamphetamine in saliva. Based on phosphor color and position in LF assays strips, drug molecules could be successfully identified; the whole test process requires a minimum of 10 min. Another example is the use of Ln-doped UCNPs in LF assays for detection of human chorionic gonadotropin (hCG) (Hampl et al., 2001). It was demonstrated that the detection limit was 10–100 pg/ml, which is at least 2 to 3 orders of magnitude higher than conventional colored latex beads or colloidal gold based LF assay. It is known that the reliability of schistosoma infections detection with enzyme-linked immunosorbent assay (ELISA) is limited due to its lack in sensitivity and robustness. Corstjens et al. (2008) recently demonstrated Ln-doped UCNPs based LF assay for schistosoma infections detection with a higher sensitivity than that associated with the standard ELISA method: the former identified 36 positive samples, compared to 15 detected by the later. More applications of Ln-doped UCNPs in the development of LF assay strips and their biomedical applications could be found in other related studies (Corstjens et al., 2001, 2003).

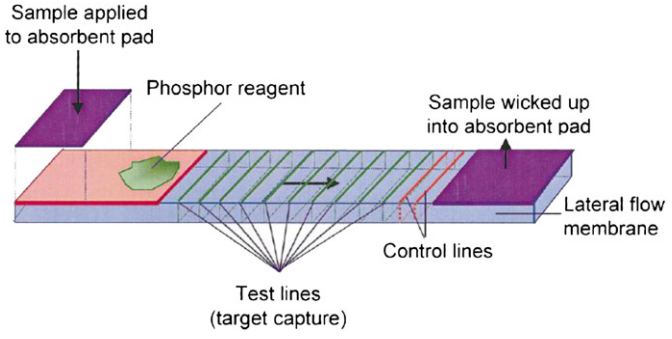


**Fig. 5.** Upconversion phosphor technology lateral flow (LF) strip format. The architecture of the LF strip is designed to accommodate up to 12 distinct test lines. In addition, each strip also contains two control lines (Niedbala et al., 2001).

The successful application of Ln-doped UCNPs in the development of LF assay strips for immunoassays implies that point-of-care detection of diseases and environmental monitoring is achievable. The techniques built upon Ln-doped UCNPs have several advantages over traditional amplification based techniques that require PCR or signal-amplification methods, in terms of cost, simplicity, portability and time saving.

### 5.4. Drug delivery

Despise superiority in bioimaging and bio-detection, Ln-doped UCNPs have been recently developed as drug carriers for cancer therapies (Qian et al., 2010b; Wang et al., 2011a; Xu et al., 2011a,b). Gai et al. (2010) demonstrated the usage of β-$NaYF_4$:Yb,Er nanoparticles in a drug delivery system. In their study, a multifunctional material $Fe_3O_4$@n$SiO_2$@m$SiO_2$@$NaYF_4$:Yb,Er was synthesized using a two-step sol–gel process. Drug release tests revealed that the upconversion luminescent intensity of the composite carrier increases with the released amount of drug due to decreasing quenching effect by the organic group from the drug. These results indicate that, by relating to the change in luminescence intensity, it is possible to quantitatively monitor the drug release process *in vivo*.

Since NIR light beam has good tissue penetration depth, photodynamic therapies (PDT) are emerging as effective treatment for cancers: upon NIR excitation, Ln-doped UCNPs emit visible light to further excite the photosensitizing drugs (Qian et al., 2009; Zhang et al., 2007) as schematically shown in Fig. 6. Excellent reviews on

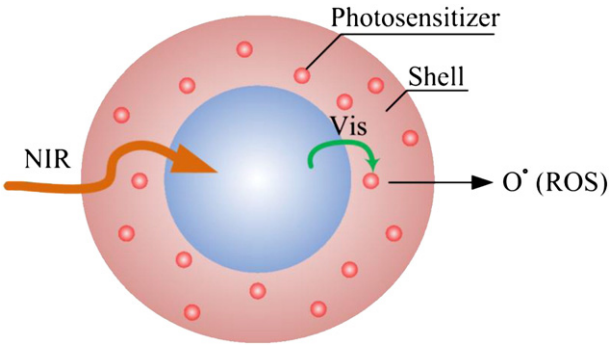


**Fig. 6.** Schematic of UCNP based drug carrier for photodynamic therapy (PDT). Upon NIR excitation, UCNPs emit visible light to further excite the photosensitizer (impregnated in the shell), resulting in the releasing of reactive oxygen species (ROS) and causing damage in nearby cancer cells.

applications of Ln-doped UCNPs in PDT have been given by Ang et al. (2011) and Wang et al. (2010a). In a typical application of UCNPs in PDT therapy, Chatterjee and Zhang (2008) attached zinc phthalocyanine (ZnPc) to polyethylenimine modified $NaYF_4$:Yb,Er nanoparticles. Since ZnPc has high absorbance of the emission from $NaYF_4$:Yb, Er nanoparticles, upon NIR irradiation, $NaYF_4$:Yb,Er nanoparticles emit visible light to photosensitize ZnPc, producing reactive oxygen species that can cause oxidative damage of cancer cells.

## 6. Concluding remarks and future directions

This article presents a state-of-the-art review on recent advances in Ln-doped UCNPs including synthetic approaches, surface modification, and biomedical applications. The relative studies continue to be a prospective and growing interdisciplinary research field that couples chemistry, materials science and engineering, biomedical science and engineering.

Though numerous achievements have been made, there still exist challenges, which hinder potential developments of practical clinical applications and point-of-care devices based on the unique optical and magnetic (or multimodal) properties of Ln-doped UCNPs. Three major topics for further studies are therefore identified as follows.

Firstly, with respect to synthetic procedures, the preparation of sub 10 nm particles is highly demanded for intracellular applications. The main problem associated with the synthesis of small size Ln-doped NCNPs is the significant reduction in luminescence efficiency. To prepare small size Ln-doped UCNPs while maintaining their luminescent intensity, advanced synthetic procedures are to be developed through adjusting reaction parameters (*e.g.*, time, temperature, concentration, pH value), selection of host matrix and dopant irons, appropriate surface coating and phase control, and so on (Qian et al., 2010b; Wang et al., 2010b; Zhang et al., 2010b).

Secondly, even though Ln-doped UCNPs possess unique properties, they could not be effectively used in many biosciences due to their dissolubility in aqueous solutions, lack of target biorecognition and bioanalytical functions. Numerous methods have been established for surface functionalization of Ln-doped UCNPs with polyacrylic acid coating, silica coating and attachment of various biomolecules such as DNA, antibody and peptides (Jiang et al., 2009; Li and Zhang, 2008; Nagarajan et al., 2010). Nevertheless, a few issues are yet addressed. For example, quantitatively controlling the amount of ligands attached on the surface and subsequently confirming the presence of biomolecules turned out to be difficult. Besides, realization of multiple functionalities *via* multiple decorating of ligands on the surface of Ln-doped UCNPs is challenging.

Thirdly, while the use of NIR for excitation of Ln-doped UCNs provides good tissue penetration depths for *in vivo* in-depth tissue imaging (Chatterjee and Zhang, 2008; Wang et al., 2011a), limitations still exist when performing *in vivo* imaging in larger animals or humans in a clinical setting. Although NIR has relatively better tissue penetration depth than UV and visible light, it is far from sufficient for whole body imaging in deep human body tissue. An alternative way to access deep tissue imaging is magnetic resonance imaging (MRI). Synthesis of nanoparticles as multimodal imaging (magnetic-fluorescent) probes has attracted attention in recent years because of their emerging potential as candidates for both optical imaging and MRI imaging at either tissue or cellular level (Carlos et al., 2011; Jańczewski et al., 2011; Li et al., 2008b; Li et al., 2009; Yallapu et al., 2011). This is a fast growing area demanding new developments in the near future, requiring more efforts devoted to the synthesis of bimodal Ln-doped UCNPs for bifunctional probes in fluorescence microscopy and MRI imaging.

## Acknowledgments

This work was supported by the Major International (Regional) Joint Research Program of China (11120101002); the National Natural Science Foundation of China (10825210); and the National 111 Project of China (B06024).

## References

Ang LY, Lim ME, Ong LC, Zhang Y. Applications of upconversion nanoparticles in imaging, detection and therapy. Nanomedicine 2011;6:1273–88.
Auzel F. Upconversion and anti-stokes processes with f and d ions in solids. Chem Rev 2004;104:139–74.
Berezin MY, Achilefu S. Fluorescence lifetime measurements and biological imaging. Chem Rev 2010;110:2641–84.
Boyer JC, Cuccia LA, Capobianco JA. Synthesis of colloidal upconverting $NaYF_4$: $Er^{3+}/Yb^{3+}$ and $Tm^{3+}/Yb^{3+}$ monodisperse nanocrystals. Nano Lett 2007;7:847–52.
Boyer JC, Manseau MP, Murray JI, van Veggel FCJM. Surface modification of upconverting $NaYF_4$ nanoparticles doped with PEG-phosphate ligands for NIR (800 nm) biolabeling within the biological window. Langmuir 2010;26:1157–64.
Boyer JC, Vetrone F, Cuccia LA, Capobianco JA. Synthesis of colloidal upconverting $NaYF_4$ nanocrystals doped with $Er^{3+}$, $Yb^{3+}$ and $Tm^{3+}$, $Yb^{3+}$ *via* thermal decomposition of lanthanide trifluoroacetate precursors. J Am Chem Soc 2006;128:7444–5.
Carlos LD, Ferreira RAS, de Zea Bermudez V, Julian Lopez B, Escribano P. Progress on lanthanide-based organic–inorganic hybrid phosphors. Chem Soc Rev 2011;40:536–49.
Chatterjee DK, Gnanasammandhan MK, Zhang Y. Small upconverting fluorescent nanoparticles for biomedical applications. Small 2010;6:2781–95.
Chatterjee DK, Rufaihah AJ, Zhang Y. Upconversion fluorescence imaging of cells and small animals using lanthanide doped nanocrystals. Biomaterials 2008;29:937–43.
Chatterjee DK, Zhang Y. Upconverting nanoparticles as nanotransducers for photodynamic therapy in cancer cells. Nanomedicine 2008;3:73–82.
Cheng L, Yang K, Li YG, Chen JH, Wang CY, Shao MW, et al. Facile preparation of multifunctional upconversion nanoprobes for multimodal imaging and dual-targeted photothermal therapy. Angew Chem 2011;123:7523–8.
Chuai XH, Zhang DS, Zhao D, Zheng K, He CF, Shi F, et al. Synthesis and characterization of $Yb^{3+}$,$Tm^{3+}$:Ba2YF7 nanocrystalline with efficient upconversion fluorescence. Mater Lett 2011;65:2368–70.
Corstjens P, Zuiderwijk M, Brink A, Li S, Feindt H, Niedbala RS, et al. Use of up-converting phosphor reporters in lateral-flow assays to detect specific nucleic acid sequences: a rapid, sensitive DNA test to identify human papillomavirus type 16 infection. Clin Chem 2001;47:1885–93.
Corstjens PLAM, van Lieshout L, Zuiderwijk M, Kornelis D, Tanke HJ, Deelder AM, et al. Up-converting phosphor technology-based lateral flow assay for detection of schistosoma circulating anodic antigen in serum. J Clin Microbiol 2008;46:171–6.
Corstjens PLAM, Zuiderwijk M, Nilsson M, Feindt H, Sam Niedbala R, Tanke HJ. Lateral-flow and up-converting phosphor reporters to detect single-stranded nucleic acids in a sandwich-hybridization assay. Anal Biochem 2003;312:191–200.
Dong NN, Pedroni M, Piccinelli F, Conti G, Sbarbati A, Ramírez-Hernández JE, et al. NIR-to-NIR two-photon excited CaF2:$Tm^{3+}$,$Yb^{3+}$ nanoparticles: multifunctional nanoprobes for highly penetrating fluorescence bio-imaging. ACS Nano 2011;5:8665–71.
Du HY, Zhang WH, Sun JY. Structure and upconversion luminescence properties of $BaYF_5$:$Yb^{3+}$,$Er^{3+}$ nanoparticles prepared by different methods. J Alloys Compd 2011;509:3413–8.
Du YP, Zhang YW, Sun LD, Yan CH. Optically active uniform potassium and lithium rare earth fluoride nanocrystals derived from metal trifluoroacetate precursors. Dalton Trans 2009:8574–81.
Ehlert O, Thomann R, Darbandi M, Nann T. A four-color colloidal multiplexing nanoparticle system. ACS Nano 2008;2:120–4.
Feng SH, Xu RR. New materials in hydrothermal synthesis. Acc Chem Res 2001;34:239–47.

Gai S, Yang P, Li C, Wang W, Dai Y, Niu N, et al. Synthesis of magnetic, up-conversion luminescent, and mesoporous core–shell-structured nanocomposites as drug carriers. Adv Funct Mater 2010;20:1166–72.
Gallini S, Jurado JR, Colomer MT. Combustion synthesis of nanometric powders of $LaPO_4$ and Sr-substituted $LaPO_4$. Chem Mater 2005;17:4154–61.
Ghosh P, de la Rosa E, Oliva J, Solis D, Kar A, Patra A. Influence of surface coating on the upconversion emission properties of $LaPO_4$:Yb/Tm core-shell nanorods. J Appl Phys 2009;105:113532.
Guo H, Li ZQ, Qian HS, Hu Y, Muhammad IN. Seed-mediated synthesis of $NaYF_4$:Yb, Er/$NaGdF_4$ nanocrystals with improved upconversion fluorescence and MR relaxivity. Nanotechnology 2010;21:125602.
Gurkan UA, Moon S, Geckil H, Xu F, Wang SQ, Lu TJ, et al. Miniaturized lensless imaging systems for cell and microorganism visualization in point-of-care testing. Biotechnol J 2011;6:138–49.
Hampl J, Hall M, Mufti NA, Yao YM, MacQueen DB, Wright WH, et al. Upconverting phosphor reporters in immunochromatographic assays. Anal Biochem 2001;288:176–87.
Heer S, Kömpe K, Güdel HU, Haase M. Highly efficient multicolour upconversion emission in transparent colloids of lanthanide-doped $NaYF_4$ nanocrystals. Adv Mater 2004;16:2102–5.
Heer S, Lehmann O, Haase M, Güdel HU. Blue, green, and red upconversion emission from lanthanide-doped $LuPO_4$ and $YbPO_4$ nanocrystals in a transparent colloidal solution. Angew Chem Int Ed Engl 2003;42:3179–82.
Hilderbrand SA, Shao FW, Salthouse C, Mahmood U, Weissleder R. Upconverting luminescent nanomaterials: application to *in vivo* bioimaging. Chem Commun 2009:4188–90.
Hu H, Xiong LQ, Zhou J, Li FY, Cao TY, Huang CH. Multimodal-luminescence core–shell nanocomposites for targeted imaging of tumor cells. Chem Eur J 2009;15:3577–84.
Huang P, Chen DQ, Wang YS. Host-sensitized multicolor tunable luminescence of lanthanide ion doped one-dimensional $YVO_4$ nano-crystals. J Alloys Compd 2010;509:3375–81.
Huang X, Neretina S, El-Sayed MA. Gold nanorods: from synthesis and properties to biological and biomedical applications. Adv Mater 2009;21:4880–910.
Idris NM, Li ZQ, Ye L, Sim EKW, Mahendran R, Ho PCL, et al. Tracking transplanted cells in live animal using upconversion fluorescent nanoparticles. Biomaterials 2009;30:5104–13.
Jaafar IH, LeBlon CE, Wei MT, Ou Yang D, Coulter JP, Jedlicka SS. Improving fluorescence imaging of biological cells on biomedical polymers. Acta Biomater 2010;7:1588–98.
Jalil AR, Zhang Y. Biocompatibility of silica coated $NaYF_4$ upconversion fluorescent nanocrystals. Biomaterials 2008;29:4122–8.
Jańczewski D, Zhang Y, Das GK, Yi DK, Padmanabhan P, Bhakoo KK, et al. Bimodal magnetic-fluorescent probes for bioimaging. Microsc Res Tech 2011;74:563–76.
Jiang S, et al. NIR-to-visible upconversion nanoparticles for fluorescent labeling and targeted delivery of siRNA. Nanotechnology 2009;20:155101.
Jiang S, Zhang Y. Upconversion nanoparticles-based FRET system for study of siRNA in live cells. Langmuir 2010;26:6689–94.
Jin JF, Gu YJ, Man CWY, Cheng JP, Xu ZH, Zhang Y, et al. Polymer-coated NaYF4:$Yb^{3+}$, $Er^{3+}$ upconversion nanoparticles for charge-dependent cellular imaging. ACS Nano 2011;5:7838–47.
Johnson NJJ, Sangeetha NM, Boye JC, van Veggel FCJM. Facile ligand-exchange with polyvinylpyrrolidone and subsequent silica coating of hydrophobic upconverting β-$NaYF_4$:$Yb^{3+}$/$Er^{3+}$ nanoparticles. Nanoscale 2010;2:771–7.
Kamimura M, Miyamoto D, Saito Y, Soga K, Nagasaki Y. Design of poly(ethylene glycol)/streptavidin coimmobilized upconversion nanophosphors and their application to fluorescence biolabeling. Langmuir 2008;24:8864–70.
Kobayashi H, Ogawa M, Alford R, Choyke PL, Urano Y. New strategies for fluorescent probe design in medical diagnostic imaging. Chem Rev 2010;110:2620–40.
Lakowicz JR. Principles of fluorescence spectroscopy. New York: Springer; 2006.
Lakshminarayana G, Qiu JR, Brik MG, Kityk IV. Photoluminescence of $Pr^{3+}$, $Dy^{3+}$ and $Tm^{3+}$ doped transparent nanocrystallized KNbGeO5 glasses. J Phys D: Appl Phys 2008;41:175106.
Larson DR, Zipfel WR, Williams RM, Clark SW, Bruchez MP, Wise FW, et al. Water-soluble quantum dots for multiphoton fluorescence imaging *in vivo*. Science 2003;300:1434–6.
Lau JSY, Lee PK, Tsang KHK, Ng CHC, Lam YW, Cheng SH, et al. Luminescent cyclometalated iridium(III) polypyridine indole complexes—synthesis, photophysics, electrochemistry, protein-binding properties, cytotoxicity, and cellular uptake. Inorg Chem 2009;48:708–18.
Li CX, Quan ZW, Yang PP, Huang SS, Lian HZ, Lin J. Shape-controllable synthesis and upconversion properties of lutetium fluoride (doped with $Yb^{3+}$/$Er^{3+}$) microcrystals by hydrothermal process. J Phys Chem C 2008a;112:13395–404.
Li ZQ, Guo HC, Qian HS, Hu Y. Facile microemulsion route to coat carbonized glucose on upconversion nanocrystals as high luminescence and biocompatible cell-imaging probes. Nanotechnology 2010;21:315105.
Li ZQ, Zhang Y. An efficient and user-friendly method for the synthesis of hexagonal-phase $NaYF_4$:Yb,Er/Tm nanocrystals with controllable shape and upconversion fluorescence. Nanotechnology 2008;19:345606.
Li ZQ, Zhang Y. Monodisperse silica-coated polyvinylpyrrolidone/$NaYF_4$ nanocrystals with multicolor upconversion fluorescence emission. Angew Chem Int Ed Engl 2006;45:7732–5.
Li ZQ, Zhang Y, Jiang S. Multicolor core/shell-structured upconversion fluorescent nanoparticles. Adv Mater 2008b;20:4765–9.
Li ZQ, Zhang Y, Shuter B, Idris M. Hybrid lanthanide nanoparticles with paramagnetic shell coated on upconversion fluorescent nanocrystals. Langmuir 2009;25:12015–8.
Liang H, Chen G, Li L, Liu Y, Qin F, Zhang Z. Upconversion luminescence in $Yb^{3+}$/$Tb^{3+}$-codoped monodisperse $NaYF_4$ nanocrystals. Opt Commun 2009;282:3028–31.
Liang S, Liu Y, Tang Y, Xie Y, Sun HZ, Zhang H, et al. A user-friendly method for synthesizing high-quality NaYF4:Yb, Er(Tm) nanocrystals in liquid paraffin. J Nanomater 2011;2011:1.
Lim SF. Upconverting nanophosphors for bioimaging. Nanotechnology 2009;20:405701.
Lim SF, Riehn R, Ryu WS, Khanarian N, Tung CK, Tank D, et al. *In vivo* and scanning electron microscopy imaging of upconverting nanophosphors in *Caenorhabditis elegans*. Nano Lett 2006;6:169–74.
Liu C, Chen D. Controlled synthesis of hexagon shaped lanthanide-doped $LaF_3$ nanoplates with multicolor upconversion fluorescence. J Mater Chem 2007;17:3875–80.
Liu S, Han MY. Silica-coated metal nanoparticles. Chem Asian J 2010;5:36–45.
Liu X, MZhao J, WSun Y, JSong K, Yu Y, Du C, et al. Ionothermal synthesis of hexagonal-phase $NaYF_4$:$Yb^{3+}$,$Er^{3+}$/$Tm^{3+}$ upconversion nanophosphors. Chem Commun 2009a;43:6628–30.
Liu YX, Pisarski WA, Zeng SJ, Xu CF, Yang QB. Tri-color upconversion luminescence of rare earth doped $BaTiO_3$ nanocrystals and lowered color separation. Opt Express 2009b;17:9089–98.
Louie A. Multimodality imaging probes: design and challenges. Chem Rev 2010;110:3146–95.
Mader HS, Kele P, Saleh SM, Wolfbeis OS. Upconverting luminescent nanoparticles for use in bioconjugation and bioimaging. Curr Opin Chem Biol 2010;14:582–96.
Mahalingam V, Naccache R, Vetrone F, Capobianco JA. Sensitized $Ce^{3+}$ and $Gd^{3+}$ ultraviolet emissions by $Tm^{3+}$ in colloidal $LiYF_4$ nanocrystals. Chem Eur J 2009;15:9660–3.
Mai HX, Zhang YW, Si RYan ZG, Sun LD, You LP, et al. High-quality sodium rare-earth fluoride nanocrystals: controlled synthesis and optical properties. J Am Chem Soc 2006;128:6426–36.
Mai HX, Zhang YW, Sun LD, Yan CH. Highly efficient multicolor up-conversion emissions and their mechanisms of monodisperse NaYF4:Yb,Er core and core/shell-structured nanocrystals. J Phys Chem C 2007;111:13721–9.
Malkani N, Schmid JA. Some secrets of fluorescent proteins: distinct bleaching in various mounting fluids and photoactivation of cyan fluorescent proteins at YFP-excitation. PLoS One 2011;6:e18586.
Medintz L, Uyeda HT, Goldman ER, Mattoussi H. Quantum dot bioconjugates for imaging, labelling and sensing. Nat Mater 2005;4:435–46.
Nagarajan S, Li ZQ, Artzner VM, Grasset F, Zhang Y. Imaging gap junctions with silica-coated upconversion nanoparticles. Med Biol Eng Comput 2010;48:1033–41.
Niedbala RS, Feindt H, Kardos K, Vail T, Burton J, Bielska B, et al. Detection of analytes by immunoassay using up-converting phosphor technology. Anal Biochem 2001;293:22–30.
Niu WB, Wu S, Zhang SF, Li J, Li L. Multicolor output and shape controlled synthesis of lanthanide-ion doped fluorides upconversion nanoparticles. Dalton Trans 2011;40:3305–14.
Ong LC, Gnanasammandhan MK, Nagarajan S, Zhang Y. Upconversion: road to El Dorado of the fluorescence world. Luminescence 2010;25:290–3.
Park YI, Kim JH, Lee KT, Jeon KS, Na HB, Yu JH, et al. Nonblinking and nonbleaching upconverting nanoparticles as an optical imaging nanoprobe and T1 magnetic resonance imaging contrast agent. Adv Mater 2009;21:4467–71.
Patra A, Friend CS, Kapoor R, Prasad PN. Fluorescence upconversion properties of $Er^{3+}$-doped $TiO_2$ and $BaTiO_3$ nanocrystallites. Chem Mater 2003;15:3650–5.
Patra A, Friend CS, Kapoor R, Prasad PN. Upconversion in $Er^{3+}$:$ZrO_2$ nanocrystals. J Phys Chem B 2002;106:1909–12.
Patra CR, Alexandra G, Patra S, Jacob DS, Gedanken A, Landau A, et al. Microwave approach for the synthesis of rhabdophane-type lanthanide orthophosphate (Ln = La, Ce, Nd, Sm, Eu, Gd and Tb) nanorods under solvothermal conditions. New J Chem 2005;29:733–9.
Piao Y, Burns A, Kim J, Wiesner U, Hyeon T. Designed fabrication of silica-based nanostructured particle systems for nanomedicine applications. Adv Funct Mater 2008;18:3745–58.
Qian HS, Guo HC, Ho PC-L, Mahendran R, Zhang Y. Mesoporous-silica-coated up-conversion fluorescent nanoparticles for photodynamic therapy. Small 2009;5:2285–90.
Qian J, Jiang L, Cai F, Wang D, He S. Fluorescence-surface enhanced Raman scattering co-functionalized gold nanorods as near-infrared probes for purely optical *in vivo* imaging. Biomaterials 2010a;32:1601–10.
Qian L, Zhou L, Too HP, Chow GM. Gold decorated $NaYF_4$:Yb,Er/$NaYF_4$/silica (core/-shell/shell) upconversion nanoparticles for photothermal destruction of BE(2)-C neuroblastoma cells. J Nanopart Res 2010b:1-12.
Qin X, Yokomori T, Ju YG. Flame synthesis and characterization of rare-earth ($Er^{3+}$, $Ho^{3+}$, and $Tm^{3+}$) doped upconversion nanophosphors. Appl Phys Lett 2007;90:073104–6.
Qiu HL, Chen GY, Sun L, Hao SW, Han G, Yang CH. Ethylenediaminetetraacetic acid (EDTA)-controlled synthesis of multicolor lanthanide doped $BaYF_5$ upconversion nanocrystals. J Mater Chem 2011;21:17202–8.
Quan ZW, Yang DM, Li CX, Kong DY, Yang PP, Cheng ZY, et al. Multicolor tuning of manganese-doped ZnS colloidal nanocrystals. Langmuir 2009;25:10259–62.
Rantanen T, Järvenpää ML, Vuojola J, Kuningas K, Soukka T. Fluorescence-quenching-based enzyme-activity assay by using photon upconversion. Angew Chem 2008;120:3871–3.
Schäfer H, Ptacek P, Zerzouf O, Haase M. Synthesis and optical properties of $KYF_4$/Yb, Er nanocrystals, and their surface modification with undoped $KYF_4$. Adv Funct Mater 2008;18:2913–8.
Shan JN, Qin X, Yao N, Ju YG. Synthesis of monodisperse hexagonal $NaYF_4$:Yb, Ln (Ln = Er, Ho and Tm) upconversion nanocrystals in TOPO. Nanotechnology 2007;18:445607.

Shan JN, Ju YG. A single-step synthesis and the kinetic mechanism for monodisperse and hexagonal-phase $NaYF_4$:Yb,Er upconversion nanophosphors. Nanotechnology 2009;20:275603.
Singh S, Singh A, Kumar D, Prakash O, Rai S. Efficient UV–visible up-conversion emission in $Er^{3+}/Yb^{3+}$ co-doped $La_2O_3$ nano-crystalline phosphor. Appl Phys B 2010;98:173–9.
Soukka T, Rantanen T, Kuningas K. Photon upconversion in homogeneous fluorescence-based bioanalytical assays. Ann N Y Acad Sci 2008;1130:188–200.
Su J, Zhang QL, Shao SF, Liu WP, Wan SM, Yin ST. Phase transition, structure and luminescence of Eu:YAG nanophosphors by co-precipitation method. J Alloys Compd 2009;470:306–10.
Su Kim J, Kyung Kwon A, Kim JS, Lee Park H, Chul Kim G, do Han S. Optical and structural properties of $ZnGa_2O_4$: $Eu^{3+}$ nanophosphor by hydrothermal method. J Lumin 2007;122–123:851–4.
Sudhagar S, Sathya S, Pandian K, Lakshmi B. Targeting and sensing cancer cells with ZnO nanoprobes *in vitro*. Biotechnol Lett 2011;33:1891–6.
Sudheendra L, Ortalan V, Dey S, Browning ND, Kennedy IM. Plasmonic enhanced emissions from cubic $NaYF_4$:Yb:Er/Tm nanophosphors. Chem Mater 2011;23:2987–93.
Tsien RY. The green fluorescent protein. Ann Rev Biochem 1998;67:509–44.
Vadivel Murugan A, Viswanath AK, Ravi V, Kakade BA, Saaminathan V. Photoluminescence studies of $Eu^{3+}$ doped $Y_2O_3$ nanophosphor prepared by microwave hydrothermal method. Appl Phys Lett 2006;89:123120–2.
van de Rijke F, Zijlmans H, Li S, Vail T, Raap AK, Niedbala RS, et al. Up-converting phosphor reporters for nucleic acid microarrays. Nat Biotechnol 2001;19:273–6.
Venkatramu V, Falcomer D, Speghini A, Bettinelli M, Jayasankar CK. Synthesis and luminescence properties of $Er^{3+}$-doped $Lu_3Ga_5O_{12}$ nanocrystals. J Lumin 2008;128: 811–3.
Vetrone F, Naccache R, Mahalingam V, Morgan CG, Capobianco JA. The active-core/active-shell approach: a strategy to enhance the upconversion luminescence in lanthanide-doped nanoparticles. Adv Funct Mater 2009;19:2924–9.
Vu N, Kim Anh T, Yi GC, Strek W. Photoluminescence and cathodoluminescence properties of $Y_2O_3$:Eu nanophosphors prepared by combustion synthesis. J Lumin 2007;122–123:776–9.
Wang C, Cheng L, Liu Z. Drug delivery with upconversion nanoparticles for multi-functional targeted cancer cell imaging and therapy. Biomaterials 2011a;32:1110–20.
Wang C, Ma Q, Dou WC, Kanwal S, Wang GN, Yuan PF, et al. Synthesis of aqueous CdTe quantum dots embedded silica nanoparticles and their applications as fluorescence probes. Talanta 2009a;77:1358–64.
Wang C, Tao HQ, Cheng L, Liu Z. Near-infrared light induced *in vivo* photodynamic therapy of cancer based on upconversion nanoparticles. Biomaterials 2011b;32: 6145–54.
Wang F, Banerjee D, Liu Y, Chen X, Liu X. Upconversion nanoparticles in biological labeling, imaging, and therapy. Analyst 2010a;135:1839–54.
Wang F, Chatterjee DK, Li ZQ, Zhang Y, Fan XP, Wang MQ. Synthesis of polyethylenimine/$NaYF_4$ nanoparticles with upconversion fluorescence. Nanotechnology 2006;17:5786.
Wang F, Han Y, Lim CS, Lu YH, Wang J, Xu J, et al. Simultaneous phase and size control of upconversion nanocrystals through lanthanide doping. Nature 2010b;463: 1061–5.
Wang F, Liu XG. Upconversion multicolor fine-tuning: visible to near-infrared emission from lanthanide-doped $NaYF_4$ nanoparticles. J Am Chem Soc 2008;130: 5642–3.
Wang F, Liu XG. Recent advances in the chemistry of lanthanide-doped upconversion nanocrystals. Chem Soc Rev 2009;38:976–89.
Wang G, Peng Q, Li Y. Upconversion luminescence of monodisperse $CaF_2$:$Yb^{3+}/Er^{3+}$ nanocrystals. J Am Chem Soc 2009b;131:14200–1.
Wang G, Peng Q, Li Y. Lanthanide-doped nanocrystals: synthesis, optical-magnetic properties, and applications. Acc Chem Res 2011c;44:322–32.
Wang L, Li Y. Green upconversion nanocrystals for DNA detection. Chem Commun 2006:2557–9.
Wang LY, Yan RX, Huo ZY, Wang L, Zeng JH, Bao J, et al. Fluorescence resonant energy transfer biosensor based on upconversion-luminescent nanoparticles. Angew Chem Int Ed Engl 2005;44:6054–7.
Wang LY, Zhang Y, Zhu YY. One-pot synthesis and strong near-infrared upconversion luminescence of poly(acrylic acid)-functionalized $YF_3$:$Yb^{3+}/Er^{3+}$ nanocrystals. Nano Res 2010c;3:317–25.
Wang M, Abbineni G, Clevenger A, Mao CB, Xu SK. Upconversion nanoparticles: synthesis, surface modification and biological applications. Nanomed Nanotechnol Biol Med 2011d;7:710–29.
Wang M, Hou W, Mi CC, Wang WX, Xu ZR, Teng HH, et al. Immunoassay of goat anti-human immunoglobulin g antibody based on luminescence resonance energy transfer between near-infrared responsive NaYF4:Yb, Er upconversion fluorescent nanoparticles and gold nanoparticles. Anal Chem 2009c;81:8783–9.
Wang M, Mi CC, Wang WX, Liu CH, Wu YF, Xu ZR, et al. Immunolabeling and NIR-excited fluorescent imaging of heLa cells by using NaYF4:Yb,Er upconversion nanoparticles. ACS Nano 2009d;3:1580–6.
Wang SQ, Esfahani M, Gurkan UA, Inci F, Kuritzkes D, Demirci U. Efficient on-chip isolation of HIV subtypes. Lab Chip 2012;12:1508–15.
Wang SQ, Ip A, Xu F, Giguel F, Moon S, Akay A. Development of a microfluidic system for measuring HIV-1 viral load. Proc SPIE Int Soc Opt Eng 2010d;7666:76661H–1.
Wang SQ, Xu F, Demirci U. Advances in developing HIV-1 viral load assays for resource-limited settings. Biotechnol Adv 2010e;28:770–81.
Wang SQ, Zhao XH, Khimji I, Akbas R, Qiu WL, Edwards D, et al. Integration of cell phone imaging with microchip ELISA to detect ovarian cancer HE4 biomarker in urine at the point-of-care. Lab Chip 2011e;11:3411–8.
Weiss S. Fluorescence spectroscopy of single biomolecules. Science 1999;283: 1676–83.
Williams R. Surface modification of biomaterials. Mater Today 2011;14:290.
Wu X, Liu H, Liu J, Haley KN, Treadway JA, Larson JP, et al. Immunofluorescent labeling of cancer marker Her2 and other cellular targets with semiconductor quantum dots. Nat Biotechnol 2002;21:41–6.
Wu XJ, Zhang QB, Wang X, Yang H, Zhu YM. One-pot synthesis of carboxyl-functionalized rare earth fluoride nanocrystals with monodispersity, ultrasmall size and very bright luminescence. Eur J Inorg Chem 2011;2011:2158–63.
Xing HY, Bu WB, Zhang SJ, Zheng XP, Li M, Chen F, et al. Multifunctional nanoprobes for upconversion fluorescence, MR and CT trimodal imaging. Biomaterials 2012;33: 1079–89.
Xing Y, Rao J. Quantum dot bioconjugates for *in vitro* diagnostics & *in vivo* imaging. Cancer Biomark 2008;4:307–19.
Xiong LQ, Chen ZG, Yu MX, Li FY, Liu C, Huang CH. Synthesis, characterization, and *in vivo* targeted imaging of amine-functionalized rare-earth up-converting nanophosphors. Biomaterials 2009;30:5592–600.
Xiong LQ, Yang TS, Yang Y, Xu CJ, Li FY. Long-term *in vivo* biodistribution imaging and toxicity of polyacrylic acid-coated upconversion nanophosphors. Biomaterials 2010;31:7078–85.
Xu ZH, Li CX, Cheng ZY, Zhang CM, Li GG, Peng C, et al. Self-assembled 3D architectures of lanthanide orthoborate: hydrothermal synthesis and luminescence properties. CrystEngComm 2010;12:549–57.
Xu ZH, Li CX, Ma PG, Hou ZY, Yang DM, Kang XJ, et al. Facile synthesis of an up-conversion luminescent and mesoporous $Gd_2O_3$:$Er^{3+}$@n$SiO_2$@m$SiO_2$ nanocomposite as a drug carrier. Nanoscale 2011a;3:661–7.
Xu ZH, Li CX, Yang PP, Hou ZY, Zhang CM, Lin J. Uniform $Ln(OH)_3$ and $Ln_2O_3$ (Ln = Eu, Sm) submicrospindles: facile synthesis and characterization. Cryst Growth Des 2009;9:4127–35.
Xu ZH, Ma PG, Li CX, Hou ZY, Zhai XF, Huang SS, et al. Monodisperse core–shell structured up-conversion $Yb(OH)CO_3$@$YbPO_4$:$Er^{3+}$ hollow spheres as drug carriers. Biomaterials 2011b;32:4161–73.
Yallapu MM, Othman SF, Curtis ET, Gupta BK, Jaggi M, Chauhan SC. Multi-functional magnetic nanoparticles for magnetic resonance imaging and cancer therapy. Biomaterials 2011;32:1890–905.
Yan ZG, Yan CH. Controlled synthesis of rare earth nanostructures. J Mater Chem 2008;18:5046–59.
Yang J, Zhang CM, Peng C, Li CX, Wang LL, Chai RT, et al. Controllable red, green, blue (RGB) and bright white upconversion luminescence of $Lu_2O_3$:$Yb^{3+}/Er^{3+}/Tm^{3+}$ nanocrystals through single Laser excitation at 980 nm. Chem Eur J 2009;15:4649–55.
Yang YM, Shao Q, Deng RR, Wang C, Teng X, Cheng K, et al. *In vitro* and *in vivo* uncaging and bioluminescence imaging by using photocaged upconversion nanoparticles. Angew Chem Int Ed 2012;51:3125–9.
Yi GS, Lu H, Zhao S, Ge Y, Yang W, Chen D, et al. Synthesis, characterization, and biological application of size-controlled nanocrystalline NaYF4:Yb, Er infrared-to-visible up-conversion Phosphors. Nano Lett 2004;4:2191–6.
Yi GS, Chow GM. Water-soluble NaYF4:Yb, Er(Tm)/NaYF4/polymer core/shell/shell nanoparticles with significant enhancement of upconversion fluorescence. Chem Mater 2007;19:341–3.
Yi GS, Chow GM. Synthesis of hexagonal-phase NaYF4:Yb, Er and NaYF4:Yb, Tm nanocrystals with efficient up-conversion fluorescence. Adv Funct Mater 2006;16:2324–9.
Yi GS, Chow GM. Colloidal LaF3:Yb, Er, LaF3:Yb, Ho and LaF3:Yb, Tm nanocrystals with multicolor upconversion fluorescence. J Mater Chem 2005;15:4460–4.
Yin A, Zhang Y, Sun L, Yan C. Colloidal synthesis and blue based multicolor upconversion emissions of size and composition controlled monodisperse hexagonal $NaYF_4$:Yb,Tm nanocrystals. Nanoscale 2010;2.
Yu M, Li F, Chen Z, Hu H, Zhan C, Yang H, et al. Laser scanning up-conversion luminescence microscopy for imaging cells labeled with rare-earth nanophosphors. Anal Chem 2009;81:930–5.
Yu MX, Zhao Q, Shi LX, Li FY, Zhou ZG, Yang H, et al. Cationic iridium(iii) complexes for phosphorescence staining in the cytoplasm of living cells. Chem Commun 2008: 2115–7.
Yu XF, Li M, Xie MY, Chen LD, Li Y, Wang QQ. Dopant-controlled synthesis of water-soluble hexagonal $NaYF_4$ nanorods with efficient upconversion fluorescence for multicolor bioimaging. Nano Res 2010;3:51–60.
Zhang C, Sun L, Zhang Y, Yan C. Rare earth upconversion nanophosphors: synthesis, functionalization and application as biolabels and energy transfer donors. J Rare Earths 2010a;28:807–19.
Zhang F, Li J, Shan J, Xu L, Zhao D. Shape, size, and phase-controlled rare-earth fluoride nanocrystals with optical upconversion properties. Chem Eur J 2009a;15: 11010–9.
Zhang F, Shi QH, Zhang YC, Shi YF, Ding KL, Zhao DY, et al. Fluorescence upconversion microbarcodes for multiplexed biological detection: nucleic acid encoding. Adv Mater 2011;23:3775–9.
Zhang H, Li Y, Ivanov IA, Qu Y, Huang Y, Duan X. Plasmonic modulation of the upconversion fluorescence in NaYF4:Yb/Tm hexaplate nanocrystals using gold nanoparticles or nanoshells. Angew Chem Int Ed Engl 2010b;49:2865–8.
Zhang P, Rogelj S, Nguyen K, Wheeler D. Design of a highly sensitive and specific nucleotide sensor based on photon upconverting particles. J Am Chem Soc 2006;128: 12410–1.
Zhang P, Steelant W, Kumar M, Scholfield M. Versatile photosensitizers for photodynamic therapy at infrared excitation. J Am Chem Soc 2007;129:4526–7.
Zhang SZ, Sun LD, Tian H, Liu Y, Wang JF, Yan CH. Reversible luminescence switching of NaYF4:Yb,Er nanoparticles with controlled assembly of gold nanoparticles. Chem Commun 2009b:2547–9.

Zhao Q, Yu MX, Shi LX, Liu SJ, Li CY, Shi M, et al. Cationic iridium(III) complexes with tunable emission color as phosphorescent dyes for live cell Imaging. Organometallics 2010;29:1085–91.

Zhou J, Yu M, Sun Y, Zhang X, Zhu X, Wu Z, et al. Fluorine-18-labeled $Gd^{3+}/Yb^{3+}/Er^{3+}$ co-doped $NaYF_4$ nanophosphors for multimodality PET/MR/UCL imaging. Biomaterials 2011;32:1148–56.

Zijlmans HJMA, Bonnet J, Burton J, Kardos K, Vail T, Niedbala RS, et al. Detection of cell and tissue surface antigens using up-converting phosphors: a new reporter technology. Anal Biochem 1999;267:30–6.

Zuiderwijk M, Tanke HJ, Sam Niedbala R, Corstjens PLAM. An amplification-free hybridization-based DNA assay to detect streptococcus pneumoniae utilizing the up-converting phosphor technology. Clin Biochem 2003;36:401–3.